Iranian Journal of Hydrogen & Fuel Cell 3(2015) 159-168

Iranian Journal of Hydrogen & Fuel Cell

IJHFC

Journal homepage://ijhfc.irost.ir

Modeling and optimization of a non-isothermal two phase flow in the cathode gas diffusion layer of PEM fuel cell

Hassan Hassanzadeh [1,*], Seyed Hadi Golkar [2]

[1] Assistant Professor, Department of Mechanical Engineering, University of Birjand, Birjand, Iran
[2] MSc Student, Department of Mechanical Engineering, University of Birjand, Birjand, Iran

Article Information

Article History:

Received:
31 October 2015
Received in revised form:
01 January 2016
Accepted:
13 January 2016

Keywords

PEM Fuel cell
Two-phase flow
Optimization
Non-isothermal.

Abstract

In this paper, a non-isothermal two-phase flow in the cathode gas diffusion layer (GDL) of PEM fuel cell is modeled. The governing equations including energy, mass, and momentum conservation equations were solved by numerical methods. Also, the optimal values of the effective parameters such as the electrodes porosity, GDL thickness and inlet relative humidity were calculated using optimization Simulated Annealing algorithms. Optimization was done by considering the fuel cell voltage as the objective function. The results show that by increasing the relative humidity of the air, the rate of evaporation in cathode GDL and temperature distribution across the fuel cell decrease. Among the different methods of optimization, the best method for two- phase flow is the SA algorithm. Optimum porosity of the electrodes, GDL thickness and relative humidity obtained were 0.44, 0.24 mm and 99%, respectively. The fuel cell power density at optimum condition increased 6% compared to the base condition. Optimization was done by Matlab software.

1. Introduction

Nowadays, PEM fuel cells are good choices for transportation applications and portable devices because of advantages such as low operating temperature, high efficiency, high power density, solid electrolyte and quick start up. Despite these advantages, heat and water management is difficult in PEM fuel cells. In this kind of fuel cell ionic conductivity of the electrolyte is extremely dependent on the water content, so fuel and oxidizer become humid before entering the fuel cell. Water transport by reactants to the fuel cell and water production due to reaction in the cathode catalyst layer provide the conditions for the occurrence of a two-phase flow. By increasing the current density and thus producing more water in the cathode catalyst, the two-phase flow prevails in the cathode GDL. The occurrence of two-phase flow in the cathode GDL reduces the effective electrode surface and increases the resistance to mass transfers; therefore, reducing the fuel cell performance. By further increasing the current density, $j > 1A/cm^2$,

*Corresponding Author's E-mail address: h.hassanzadeh@birjand.ac.ir

the amount of water transported and produced in the cathode catalyst is also increased. By increasing the water the pores of the electrode, especially those closer to the cathode catalyst layer, are occupied by liquid water and a flooding phenomenon occurs. Since flooding can occur at high current density in the cathode GDL and also at low current density under certain operating conditions in the anode GDL [1], two-phase flow modeling is necessary.

The older models are single-phase. In these models, it is assumed that liquid water and gas mixture are transported from separate paths without contact and mass exchange [2-6]. These models can accurately predict the behavior of PEM fuel cells at low current density, but not at high current densities where real fuel cells work. Also, by increasing the current density more heat is generated by the reactions, activation and ohmic losses increase, and the temperature gradient within the fuel cell increases. Therefore, it is necessary that the effects of temperature gradient on two-phase flow parameters are studied.

In the last decade various two-phase models have been developed to consider many aspects of fuel cells [7-12]. Pasaogullari and Wang [7] in an isothermal, one dimensional and analytical two-phase model investigated water flooding and the effect of the saturation on a fuel cell performance. Zhan et al. [8] in an isothermal and one-dimensional two phase model investigated the effect of non-uniformity of porosity of the GDL on fuel cell performance. Vynnycky [9] provided a more accurate model for two-phase flow using single-phase flow equations for single-phase regions and two-phase flow equations for two-phase regions. Shi et al. [10] in a two-phase, non-isothermal and one-dimensional model considered the contact effect between two phases and introduced the saturation parameter s. They investigated the capillary pressure curve along the cathode GDL. Hassanzadeh et al. [11, 12] presented two-phase flow models with an emphasis on the effect of water flux through the membrane on the fuel cell performance.

Although, two-phase flow modeling more accurately shows fuel cell performance at certain conditions, this does not mean that the fuel cell has the best performance. So the optimization of geometric parameters and operating conditions is essential to increase efficiency and durability, and to reduce production costs. According to various geometric and operating parameters of fuel cells and the effects on performance, determination of the optimal point of a fuel cell is very important.

Susai et al. [16] have studied the effect of different membrane thickness and humidity on the performance of PEM fuel cells and have obtained optimum values of fuel cell operating conditions such as temperature of input humid air and input water vapor activity. Grujicic et al. [17, 18] obtained the optimum values of cathode thickness, width and thickness of the cathode gas channel by applying a nonlinear constrained optimization method. They investigated the optimal values of operating conditions (inlet air pressure to the cathode) by choosing the current density as an objective function. Mishra et al. [19] presented a two-phase non-isothermal and one-dimensional model for PEM fuel cell. They obtained optimum values of fuel cell operating conditions and geometrical parameters. In their work, the current density is chosen as an objective function and optimum values of input gas temperature, relative humidity and the membrane thickness were obtained. Das et al. [20] investigated the effective parameters on fuel cell performance according to an analytical study. These researchers did the optimization based on the maximum current density at constant voltage (power density as an objective function), and they have obtained optimum values of platinum and catalyst layer thicknesses. Dokkar et al. [21] investigated the optimization of the two-phase flow regime in a PEM fuel cell.

In the present paper, a non-isothermal two phase flow model was developed to study and optimize the PEM fuel cell performance. The optimum value of the geometric parameters (anode and cathode GDL thicknesses and porosity of the anode and cathode electrodes) and inlet relative humidity to the cathode were calculated using innovative optimization algorithms such as the Genetic Algorithm (GA), Simulated Annealing (SA), and Pattern Search Algorithm (PSA). Optimization was done by Matlab

optimization toolbox.

2. Assumptions

The present model is one-dimensional, steady state, non-isothermal and non-isobaric. The gas mixture is ideal and the flow is considered incompressible. The catalyst layers are assumed interface, so the electrochemical reactions occurred at the catalyst layers GDLs interface. The structures of the GDLs are assumed homogenous. There is a local thermodynamic equilibrium between the three phases including solid, liquid water, and gas mixture. In the practical current density range the flow in the cathode GDL is two-phase, but the flow in the other components of the fuel cell is single-phase.

3. Governing equations

The governing equations include the conservation equations of mass, momentum and energy, and the auxiliary equations. A number of these equations have been provided for the cathode GDL and the equations for other components can be found in [13].

Oxygen is not consumed in the cathode GDL; so change of its flux along the GDL is zero [12]:

$$\frac{d}{dz}(\rho_{mix}U_g Y_{O_2} - \varepsilon\rho_{mix}(1-s)D_{O_2}^{eff}\frac{dY_{O_2}}{dz}) = 0 \quad (1)$$

Where, ρ_{mix} and U_g represent the density and apparent velocity of the gas mixture, respectively. Furthermore, Y_{O_2} is the mass fraction of oxygen, ε is the porosity, and s is the saturation quantity that represents the fraction of GDL pores that is occupied by liquid water. The flow in the cathode GDL is two-phase, so there is contact and mass exchange between the liquid water and gas mixture. Unlike oxygen, the mass fluxes of liquid water and water vapor are changed along the cathode GDL as follows:

$$\frac{d}{dz}(\rho_{mix}U_g Y_{H_2O} - \varepsilon\rho_{mix}(1-s)D_{H_2O}^{eff}\frac{dY_{H_2O}}{dz}) = -\dot{m}''_{H_2O} \quad (2)$$

$$\frac{d}{dz}(\rho_l U_l) = \dot{m}''_{H_2O} \quad (3)$$

Where, $\dot{m}''_{H_2O}$ represents the conversion rates of water vapor to liquid water per unit volume. Also, ρ_l is the liquid water density and U_l is the apparent velocity of liquid water in the porous media.

If the water vapor mole fraction is more than its saturation value, water condensation occurs and its flux is calculated as follows [12]:

$$\dot{m}''_{H_2O} = k_{cond}\varepsilon(1-s)\frac{M_{H_2O}p_g}{RT}(X_{H_2O} - X_{H_2O}^{sat}) \quad (4)$$

Conversely, if the water vapor mole fraction is less than its saturation value, evaporation occurs and its flux is calculated as follows [12]:

$$\dot{m}''_{H_2O} = k_{vap}\varepsilon s\rho_l p_g(X_{H_2O} - X_{H_2O}^{sat}) \quad (5)$$

Where in equations (4) and (5), X_{H_2O} is the water vapor mole fraction, $X_{H_2O}^{sat}$ is the saturation water vapor mole fraction, k_{cond} is the water vapor condensation constant, k_{vap} is the water evaporation constant, P_g is the gas mixture pressure and R is the universal gas constant.

Because the flow in the cathode GDL is two-phase, a part of the GDL pores is occupied by liquid water, so the effective area of GDL for species transporting is decreased. In this situation, the apparent velocity of the liquid water and the gas mixture must be calculated by means of modified Darcy's law [12]:

$$U_l = \frac{-k_{abs}s^3}{\mu_L}\frac{dp_l}{dz} \quad (6)$$

$$U_g = \frac{-k_{abs}(1-s)^3}{\mu_g}\frac{dp_g}{dz} \quad (7)$$

Where in equations (6) and (7), and are the liquid pressure and the gas mixture pressure in the two-phase flow, respectively. The difference between liquid and gas mixture pressures is called the capillary pressure. In the porous media with a very small radius, capillary pressure is considerable. Capillary pressure cannot be calculated from the equations of capillary tubes, $p_c = 2\delta\cos(\theta)/r$, at static condition because the physics of the problem is different with the flow in porous media. Therefore, due to tortuosity of paths and variable radius of pores, use of more accurate relations is necessary. The Leverett equation is one of the most important empirical equations used for this purpose:

$$P_c = \delta\cos\theta\left(\frac{\varepsilon}{k_{abs}}\right)^{0.5} j(s) \tag{8}$$

According to this equation, capillary pressure depends on saturation , water contact angle surface θ, porosity ε, absolute permeability k_{abs}, and surface tension δ. In equation (8), *j(s)* depends on the hydrophilic and hydrophobic nature of surfaces. Figure 1 shows the distribution of *j(s)* for the two cases of hydrophilic and hydrophobic surface as a function of saturation *s*.

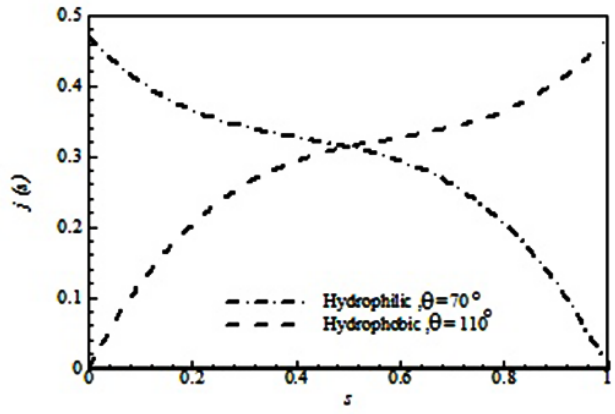

Fig. 1. Distributions of *j(s)* for hydrophilic and hydrophobic surfaces.

By assuming local thermodynamic equilibrium between the three phases (including solid, liquid water, and gas mixture), the energy equation for cathode GDL is obtained from equation (9):

$$\frac{d}{dz}\left[-(s\varepsilon k_l + (1-s)\varepsilon k_g + (1-\varepsilon)(k_s))\frac{dT}{dz}\right] + \left[\rho_l U_l c_l + \rho_g U_g c_g\right]\frac{dT}{dz} = h_{vap}\dot{m}''_{H_2O} + \dot{q} \tag{9}$$

Where, k_g, k_j, and k_s are the thermal conductivity of gas mixture, liquid water, and solid phases respectively; c_g and c_l represent the specific heat capacity of the gas mixture and liquid water, respectively; h_{vap} is the enthalpy of vaporization and $\dot{q}$ is the heat source due to ohmic losses.

4. Boundary conditions

To use more accurate boundary conditions, other fuel cell components including the membrane, anode GDL and catalyst layers are modeled. So according to the solution domain, only the boundary condition at the interface of the cathode and anode GDL and their channels are required. In practical current density range (j>0.6A/cm^2) due to the increased transfer of liquid water from the anode to the cathode and the increased generation of water in the cathode catalyst, the flow in the anode GDL is single-phase, and in the cathode GDL it is two-phase. All boundary conditions are presented in Table 1.

Table 1. Boundary Conditions

Title	Symbol	The cathode channel	The anode channel
Saturation	s	0.05	-
Gases temperature	T (K)	333	333
Relative humidity (%)	RH (%)	85	75
Gas mixture pressure	P (atm)	5	3

5. Solution and Validation

The governing equations for the two-phase flow in the cathode GDL and the single-phase flow equations for the other fuel cell components were solved by

numerical methods. The solution method and the flowchart are given in the Ref. [13]. Firstly, some calculations with different numbers of grid points were carried out to choose the suitable mesh in the cathode GdL. The results are shown in Table 2. The table shows that the calculated saturation, s, did not change significantly when the number of grid point increased beyond 15; so, from a network with 20 nodes for the cathode GDL and from 52 node for the rest of the fuel cell was used.

Table 2. The Effect of Grid Size on Saturation(s)

Nodes	s, cathode GDL
5	0.0890
10	0.0862
15	0.0854
20	0.0850
30	0.0850

Secondly, based on the boundary conditions given in Table 3, the fuel cell performance curve was compared with experimental data. As shown in Figure 2, the present numerical results are in good agreement with the experimental data of Ref. [14].

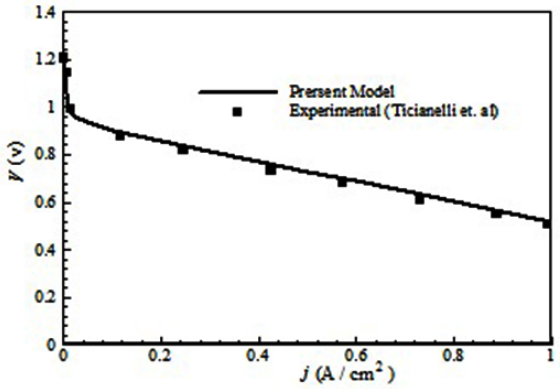

Fig. 2. Comparison between the model predictions [12] and experimental data of Ticianelli et al. [14].

finally taking into account both the effects $(\dot{m}'', s \neq 0)$. As shown in this figure, due to the reaction relative humidity has the highest value in the cathode GDL and catalyst layer interface. When considering only the contact between the two phases, the relative humidity is slightly more than the single-phase value. If both contact and mass exchange are considered, the result of two-phase flow is significantly different from the single-phase solution. Therefore for two-phase flow modeling, it is necessary to consider both the effects

Table 3. Base Values [15]

Title	Symbol	Value
Input gases temperature to the channels	T (K)	333
Input gases pressure to the anode channel	p (atm)	3
Input gases pressure to the cathode channel	p (atm)	5
GDLs thickness	t_e (μm)	300
Membrane thickness	t_m (μm)	175
GDLs and membrane porosity	ε	0.4
Relative humidity of anode channel	RH (%)	75
Relative humidity of cathode channel	RH (%)	85

6. Modeling Results

Figure 3 shows the distribution of relative humidity (RH) along the cathode GDL at different conditions: considering just the effect of contact between two phases $(\dot{m}'' = 0)$, considering just the effect of mass exchange between two phases $(s = 0, \dot{m}'' \neq 0)$, and of contact and mass exchange between the two phases. Figure 4 shows the distribution of saturation along the cathode GDL for different current densities. It is assumed that the value of saturation s in the interface of the cathode channel and cathode GDL has a fixed value of 0.05 [13]. As shown in the figure, salutation quantity changes along the cathode GDL, so the

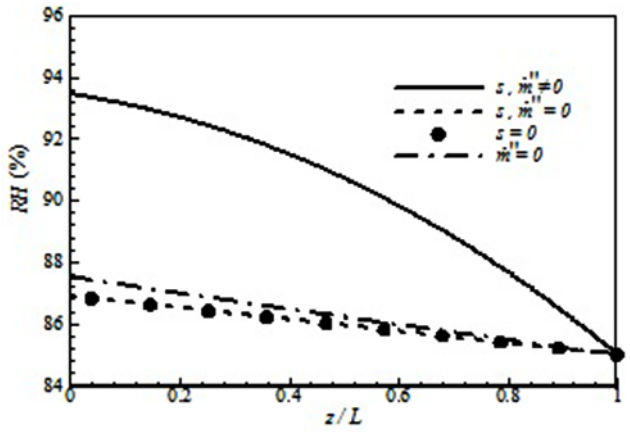

Fig. 3. The distribution of relative humidity along the cathode GDL at 100% and 85% relative humidity in anode and cathode channels, respectively.

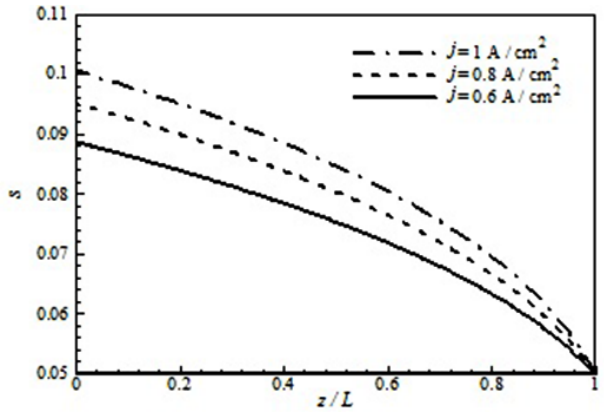

Fig. 4. Distribution of saturation along the cathode GDL for different current densities.

porosity of cathode GDL changes as $\varepsilon(z) = \varepsilon - s(z)$. As the current density increases, due to increased liquid water transfer from the anode to the cathode and more generation of water in the cathode catalyst, the saturation *s* increases along the cathode GDL.

In Figure 5, the distribution of evaporation and condensation is shown along the cathode GDL for different values of relative humidity. The evaporation rate is positive near the relative humidity of 100%, which means that condensation occurs in the cathode gas diffusion layer. This rate is reduced when it is close to the cathode channel. If the input relative humidity to the cathode is less than the saturation value, evaporation occurs and the evaporation rate is negative. According to Figure 5, the evaporation rate increased when the relative humidity in the cathode channel decreased.

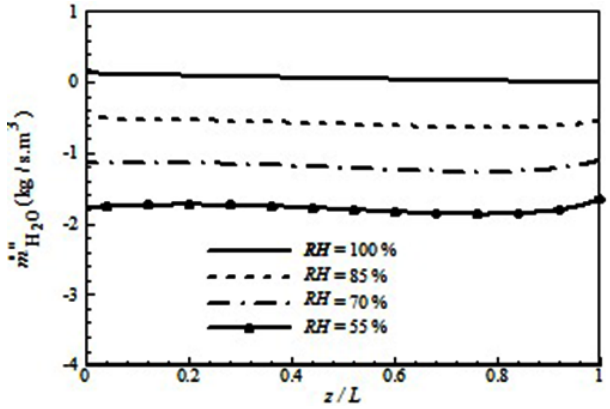

Fig. 5. Distribution of water evaporation rate in the cathode GDL for different values of relative humidity in the cathode channel.

Figure 6 shows the temperature distribution of the fuel cell at different values of relative humidity in the cathode channel. According to this figure by increasing the relative humidity the temperature distribution in the fuel cell is reduced. Increasing the relative humidity increases the water content in the membrane; therefore, the ohmic loss of membrane is decreased.

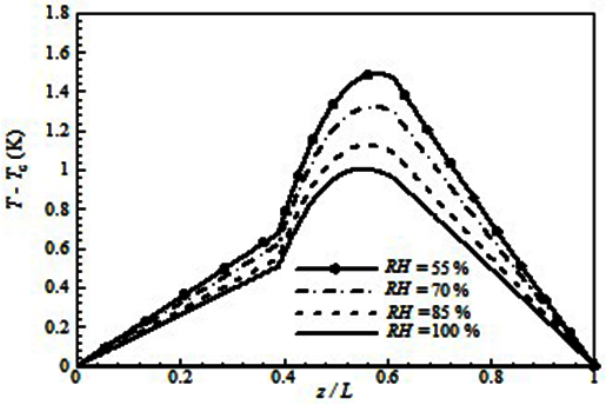

Fig. 6. Temperature distribution curve in the fuel cell for different relative humidity in the cathode channel.

7. Optimization

Using the optimization methods in engineering to find the optimum design conditions leads to lower costs and the best expected conditions are achieved.

Therefore, for commercialization of fuel cells optimization must be done to obtain competitive costs with other energy converters. For this purpose the effective parameters on fuel cell performance should be optimized. These parameters include geometric and working parameters. Geometric parameters are the thickness of the membrane, GDL thickness, porosity, the size of channels, etc., and the working parameters are the relative humidity, temperature, pressure, etc. Optimization of geometrical and performance parameters is essential in order to improve fuel cell performance, durability and lower production costs.

Finding the optimum parameters by the experimentation is time-consuming and costly. As a result it is desirable to conduct optimization numerically. The first step for optimization is the selection of goal function and the optimization variables. Depending on the aim of researchers the selection of goal function and the optimization variables are different. Table 4 shows the goal function and the optimization variables in a numbers of papers.

Table 4. Goal function and the Optimization Variables in a number of Papers

Researchers	Goal function	Optimization variables
Grujicic et al. [18,19]	v (V) at constant j	$(p_{inlet.}, \mathrm{H}_{channel}, W_{channel}, L_{GDL})_{cathode}$
Mishra et al. [20]	j(A/cm^2) at constant V	$T_{inlet,gas}, Rh, t_m, \mathrm{m}_{pt}$
Dokkar et al. [22]	$\eta_{fc,system}$, MEA total active area	$p_{inlet,gas}, j, \zeta_{H_2,\mathrm{O}_2}, \mathrm{RH}_{Channels}$

In this paper, similar to [18, 19], the output voltage at constant current density was selected as the goal function. The optimization variables were selected so that the triple voltage loss in the fuel cell is minimal. Among the different variables of fuel cells, porosity is one of the most sensitive and important parameters in that porosity variation can change some of the performance parameters of the fuel cell. In addition, relative humidity input to the cathode channel is the most important parameter for the control and management of water in a PEM fuel cell. The thickness of GDL affects the triple losses and fuel cell performance. Therefore, in this study the porosity of the anode and cathode GDL, relative humidity input to the cathode, and GDL thickness of the cathode and anode were chosen as optimization variables. So the goal function can be written as:

$$V = f[\mathrm{x}(1), \mathrm{x}(2), \mathrm{x}(3)] \quad (10)$$

Where, V is the voltage of the fuel cell and x represents the optimization parameters. In this paper we use different optimization algorithms such as Genetic Algorithms, the Simulated Annealing algorithm, and the Pattern Search Algorithm to find the optimum values. The main reason for using these algorithms is their ability to find the absolute optimum value of a function. In order to compare the results and identify the best algorithm to optimize the two-phase flow, one of the gradient methods (Fmincon) has been used to find the optimum values.

8. Optimization results

In Table 5, the runtime, stop reason and the number of iterations for optimization algorithms are compared. According to the different nature of these algorithms an exact comparison is difficult, but they can be compared in terms of the number of iterations, runtime and convergence. Among the different methods the Simulated Annealing Algorithms (SAM) was chosen as the best method to optimize the two-phase flow parameters. Using SMA in hybrid with pattern search or Fmincon slightly decreases the number of iterations but increases the program runtime.

In table 6, the optimization variables ($\mathrm{L}_{\mathrm{GDL}}$, and RH),

their ranges and their optimum values are given. Optimization was done at the current density of 1A/cm^2. Based on the optimum value, the maximum output fuel cell voltage obtained was 0.533V, so at this current density the maximum power density was 0533 W/cm^2.

Table 5. Comparison of Runtime, Stop reason, and Number of Iteration for Different Optimization Algorithm

Optimization algorithm	Stop reason	Iteration number	Runtime (s)
Genetic without hybrid function	Function Tolerance	41	615
Genetic with pattern search (hybrid)	Function Tolerance	32	520
Genetic with Fmincon (hybrid)	Function Tolerance	32	505
Simulated annealing without hybrid function	Function Tolerance	104	277
Simulated annealing with pattern search (hybrid)	Function Tolerance	104	332
Simulated annealing with Fmincon (hybrid)	Function Tolerance	104	334
Pattern search	Mesh Tolerance	51	420
Fmincon	Function Tolerance	11	250

Table 6. The optimization variables, their ranges and their optimum values

Variables	Ranges	Optimum value
L_{GDL} (mm)	$0.1< L_{GDL} <0.4$	0.24
ε_{GDL}	$0.28< \varepsilon <0.8$	0.44
Cathode RH%	50< RH<100	0.99

In Figure 7 the output voltage curve of the fuel cell is drawn for different cathode and anode electrode porosity. According to this figure the optimum porosity is 0.44. The difference between the base condition and the optimum porosity is 10%. The output voltage of the fuel cell significantly increases because a sharp drop occurs in concentration and activation losses, but the increase in the ohmic loss is not considerable. For porosity of more than 0.44, the output voltage of the fuel cell begins to decrease with a gentle slope due to increases in the ohmic losses for this range of porosity changes.

In Figure 8 the distribution of output voltage of fuel cell is drawn for the different gas diffusion layers thickness. As shown in this figure, the value of optimum GDL thickness obtained is 0.24 mm. The difference between the base and optimum values for the thickness of the GDL is 25%. By changing the thickness of GDL from 0.1 to 0.24 mm, the output voltage of the fuel cell increases because at this condition the ohmic and concentration losses are higher than the activation loss. For this reason, decreases in the ohmic and concentration losses are more than increases in the activation loss; therefore, the output voltage of the fuel cell increases.

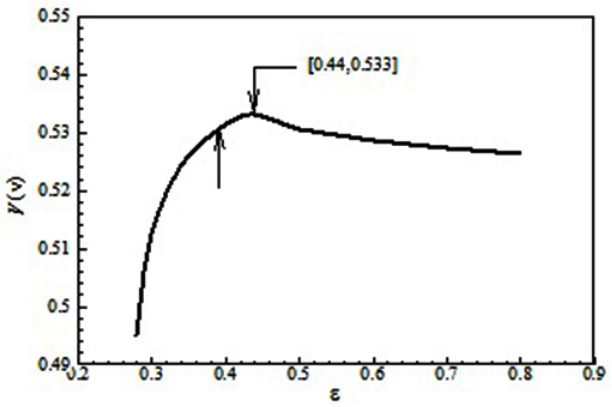

Fig. 7. Distribution of the output voltage of the fuel cell for different values of electrode porosity.

For thickness greater than 0.24 mm the distribution of output voltage is different and its value decreases because activation loss increases and the concentration and ohmic losses slightly change.

In Figure 9, the performance and power density curves of the fuel cell are compared for optimum value (Table 4) and base conditions (Table 3) at a current density of 1A/cm^2. In the optimization condition (and at a current density of 1A/cm^2) the voltage and power density are 0.533 V and 0.533 W/cm^2, respectively. As shown in Figure 9, due to using the optimum value for porosity, Rh cathode channel, and GDL thickness the output voltage and power density of the fuel cell at

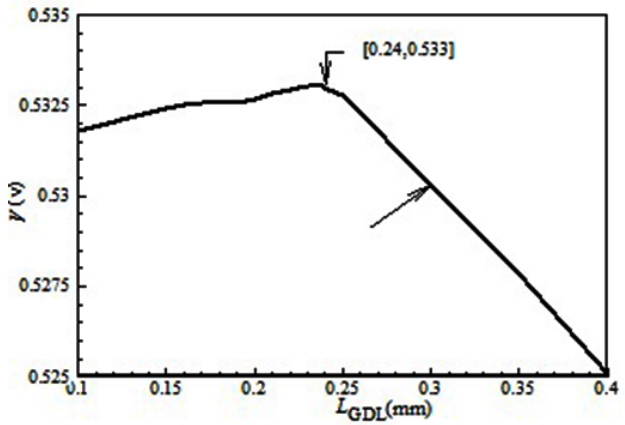

Fig. 8. Distribution of output voltage of the fuel cell for different values of GDL thickness.

optimum conditions increased 6% relative to the base case condition.

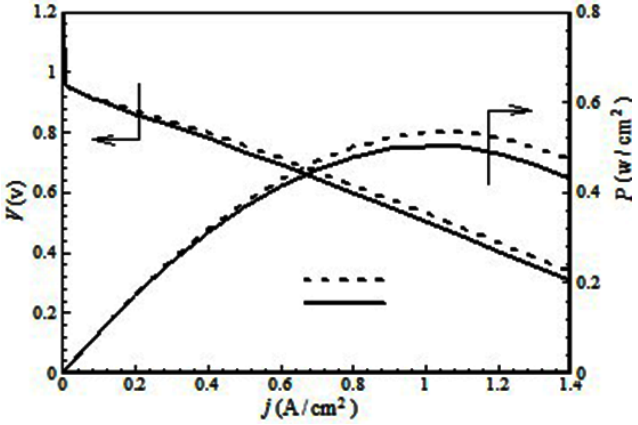

Fig. 9. Comparison of the performance and power density curves of the fuel cell in base and optimum conditions.

9. Conclusion

In this paper a non-isothermal and two-phase flow in the cathode GDL of a PEM fuel cell was modeled and optimized. The output voltage at constant current density (1A/cm^2) was selected as goal function and the optimum values of some effective parameters (including the porosity of the anode and cathode GDLs, relative humidity input to the cathode channel, and GDL thickness of the cathode and anode) were obtained by using different optimization algorithms. The results show that:

• If the relative humidity of the gases entering the cathode are in saturation condition condensation occurs in the cathode diffusion layer, and decreasing the relative humidity of the air reduces the evaporation rate.
• Increasing the current density increases the saturation in the cathode GDL.
• In optimum solution, the output voltage and power density of the fuel cell obtained were 0.533 V and 0.533 W/cm^2, respectively.
• Optimum values of porosity and thickness of the anode and the cathode GDLs and relative humidity of the cathode channel obtained were 0.44, 0.24 mm and 99%, respectively.
• SMA was the best method to optimize the two-phase flow parameters, because of shorter runtime and less dependence on the first guess.
• Fuel cell power density at optimum solution increased 6% in comparison with the base condition.

10. References

[1] Ji M. and Wei Z., "A Review of Water Management in Polymer Electrolyte Membrane Fuel Cells", Energies, 2009, 2: 1057.

[2] Bernardi D. M. and Verbrugge M. W., "Mathematical Model of a Gas Diffusion Electrode Bonded to a Polymer Electrolyte", Journal of AIChE, 1991, 37: 1151.

[3] Bernardi D. M. and Verbrugge M. W., "A Mathemathical Model of the solid-polymer-electrolyte fuel cell", Journal of The Electrochemical Society, 1992, 139: 2477

[4] Rowe A. and Li X., "Mathematical Modeling of proton exchange membrane fuel cells", Journal of Power Sources, 2001, 102: 82.

[5] Djilali N. and Lu D., "Influence of heat transfer on gas and water transport in fuel cells", International Journal of Thermal Science, 2002, 41: 20.

[6] Afshari E. and Jazayeri S. A., "Heat and Water Management in PEM Fuel Cell", Journal of WSEAS Transactions on fluid mechanics, 2008, 3: 137.

[7] Pasaogullari U. and Wang C. Y., "Liquid Water Transport in Gas Diffusion Layer of Polymer Electrolyte Fuel Cells", Journal of The Electrochemical Society, 2004, 151: 399.

[8] Zhan Z., Xiao J., Li D., Pan M. and Runzhang Y., "Effects of porosity distribution variation on the liquid water flux through gas diffusion layers of PEM fuel cells", Journal of Power Sources, 2006, 160: 1041.

[9] Vynnycky M., "On the modeling of two-phase flow in the cathode gas diffusion layer of a polymer electrolyte fuel cell", Applied Mathematical and Computation, 2007, 189: 1560.

[10] Shi W., Kurihara E. and Oshima N., "Effects of capillary pressure on liquid water removal in the cathode gas diffusion layer of a polymer electrolyte fuel cell", Journal of Power Sources, 2008, 182: 112.

[11] Hassanzadeh H., Ferdowsara A. and Barzgary M., "Modeling of two phase flow in the cathode of gas diffusion layer of proton exchange membrane fuel cell", Modares Mechanical Engineering, 2014, 14: 55 (In Persian).

[12] Hassanzadeh H., Golkar S. H. and Barzgary M., "Modeling of two phase and non - isothermal flow in polymer electrolyte fuel cell", Modares Mechanical Engineering, 2015, 15: 313 (In Persian).

[13] Golkar S. H., "Two phase and non-isothermal modeling and optimization of PEM Fuel cell", M sc. Thesis, University of Birjand, 2014, (In Persian).

[14] Ticianelli E. A., Derouin C. R., Redondo A. and Srinivasan S., "Methods to Advance Technology of Proton Exchange Membrane Fuel Cells", Journal of The Electrochemical Society, 1988, 135: 2209.

[15] Song D., Wang Q., Liu Z. S. and Huang C., "Transient analysis for the cathode gas diffusion layer of PEM fuel cells", Journal of Power Sources, 2006, 159: 928.

[16] Susai T., Kaneko M., Nakato K., Isono T., Hamada A. and Miyake Y., "Optimization of proton exchange membranes and humidifying conditions to improve cell performance polymer electrolyte fuel cells", International Journal of Hydrogen Energy, 2001, 26: 631.

[17] Grujicic M., Zhao C. L., Chittajallu K. M. and Ochterbeck J. M., "Cathode and interdigitated air distributor geometry optimization in polymer electrolyte membrane (PEM) fuel cells", Materials science and Engineering, 2004, 108: 241.

[18] Grujicic M. and Chittajallu K. M., "Design and optimization of polymer electrolyte membrane (PEM) fuel cells", Applied Surface Science, 2004, 227: 56.

[19] Mishra V., Yang F. and Pitchumani R., "Analysis and design of PEM fuel cells", Journal of Power Sources, 2005, 141: 47.

[20] Das P. K., Li X. and Liu Z., "Analytical approach to polymer electrolyte membrane fuel cell performance and optimization", Journal of Electroanalytical Chemistry, 2007, 604: 72.

[21] Dokkar B., Chennouf N., Settou N., Negrou B. and Benmhidi A., "Analysis and optimization of PEM fuel cell biphasic model", International Journal of Chemical, Materials Science and Engineering, 2013, 7: 24.